# New Constraints on Methane Fluxes and Rates of Anaerobic Methane Oxidation in a Gulf of Mexico Brine Pool via In Situ Mass Spectrometry

# New constraints on methane fluxes and rates of anaerobic methane oxidation in a Gulf of Mexico brine pool via *in situ* mass spectrometry

**Scott D. Wankel[1], Samantha B. Joye[2], Vladimir A. Samarkin[2], Sunita R. Shah[3], Gernot Friederich[4], John Melas-Kyriazi[5], and Peter R. Girguis[1*]**

[1]Department of Organismic and Evolutionary Biology, Harvard University, Cambridge, MA 02138.
[*]Corresponding author: pgirguis@oeb.harvard.edu
[2]Department of Marine Sciences, University of Georgia, Athens, GA 30602-3636
[3]US Naval Research Laboratory, Washington DC 20375
[4]Monterey Bay Aquarium Research Institute, Moss Landing, CA
[5]Stanford University, Stanford, CA 94305

**Abstract**

Deep sea biogeochemical cycles are, in general, poorly understood due to the difficulties of making measurements *in situ*, recovering samples with minimal perturbation and, in many cases, coping with high spatial and temporal heterogeneity. In particular, biogeochemical fluxes of volatiles such as methane remain largely unconstrained due to the difficulties of accurate quantification *in situ* and the patchiness of point sources such as seeps and brine pools. To better constrain biogeochemical fluxes and cycling, we have developed a deep sea *in situ* mass spectrometer (ISMS) to enable high-resolution quantification of volatiles *in situ*. Here we report direct measurements of methane concentrations made in a Gulf of Mexico brine pool located at a depth of over 2300m. Concentrations of up to 33mM methane were observed within the brine pool, while concentrations in the water directly above were three orders of magnitude lower. These direct measurements enable the first accurate estimates of the diffusive flux from a brine pool, calculated to be 1.1 ± 0.2 mol $m^{-2}$ $yr^{-1}$. Integrated rate measurements of aerobic methane oxidation in the water column overlying the brine pool were ~320 μmol $m^{-2}$ $yr^{-1}$, accounting at most for just 0.03% of the diffusive methane flux from the brine pool. Calculated rates of anaerobic methane oxidation were 600 to 1200 μM $yr^{-1}$, one to two orders of magnitude higher than previously published values of AOM in anoxic fluids. These findings suggest that brine pools are enormous point sources of methane in the deep sea, and may, in aggregate, have a pronounced impact on the global marine methane cycle.

## Introduction

### *1.1. Global importance of methane*

The marine methane cycle has been the subject of much investigation in recent years, in large part due to burgeoning interest and concern over deep ocean methane hydrates. The deep ocean methane reservoir represents an enormous and dynamic pool of carbon likely exceeding reserves of conventional oil and gas (Collett and Kuuskraa, 1998). In deep ocean regions, characterized by low temperatures, high pressure and sufficient methane concentration, methane exists largely in the solid form of a gas hydrate (Kvenvolden, 1993). Methane seeps and associated gas hydrates have been identified along many passive and active continental margins (Kvenvolden and Lorensen, 2008). Because the destabilization of hydrates is sensitive to increases in temperature or decreases in pressure, it has been postulated that increases in mean global temperatures might trigger a release of methane into the ocean and atmosphere. A significant release of methane into the atmosphere could ultimately lead to a catastrophic greenhouse effect; this mechanism has been invoked as an explanation for past deglaciation events (Dickens, 2003; Sloan *et al.*, 1992; Zachos *et al.*, 2001).

Despite recent, numerous studies of methane hydrates, modern fluxes of methane from the deep sea into surface waters and ultimately the atmosphere are very poorly constrained. Estimates of methane flux have been aided, to some degree, by recent advances in our understanding of marine microbiological influences on the global methane cycle. Aspects of the marine methane cycle remain largely unconstrained due to limitations in methods and technologies that enable accurate assessment of methane

89 concentration and flux – as well as rates of biological methanogenesis or methanotrophy.
90 Pressure and temperature have a pronounced effect on methane solubility. As such,
91 upon retrieval of methane-saturated waters or hydrate-rich sediments from the deep
92 ocean, methane rapidly outgasses to the atmosphere. Thus, it has been challenging to
93 constrain flux and microbial activity *in situ*, under environmentally relevant conditions.
94 Because previous data have shown that methane oxidation, both aerobic and anaerobic,
95 are the largest methane sinks in marine environments (Reeburgh, 2007), understanding
96 what controls methane oxidation -including concentration and abiotic flux- are paramount
97 to understanding global methane dynamics.

98 To better constrain the methane flux in chemically reducing environments – and
99 ultimately to quantify the influence of biotic and abiotic processes on the methane cycle –
100 we employed a newly developed *in situ* mass spectrometer (ISMS) to conduct direct
101 measurements of methane concentration which - in concert with shipboard
102 microbiological measurements - were used to generate more robust estimates of diffusive
103 flux and net methane oxidation rates in a newly discovered brine pool in the Gulf of
104 Mexico.

105 **2. Geologic Setting**

106 Along the continental shelf in the Gulf of Mexico, massive reservoirs of liquid
107 and gaseous hydrocarbons lie buried beneath kilometers of sediment accumulated from
108 the Mississippi River drainage basin. Due to compression and dewatering of the
109 overlying sediments, underlying evaporite deposits have undergone plastic deformation
110 resulting in salt-diapir driven tectonic activity (Kennicutt *et al.*, 1988). The resulting
111 system of fractures and faults provides conduits for the emission of hydrocarbons to the

112 seafloor via seepage (Roberts and Carney, 1997). Hydrocarbon seeps are often
113 characterized by abundant chemosynthetic based macro- and microfaunal communities
114 including tubeworms, mussel beds, and bacterial mats which thrive on the reduced
115 organic compounds emanating from below (Fisher *et al.*, 2007; MacDonald *et al.*, 1990;
116 MacDonald *et al.*, 2003). In addition, hypersaline brine fluids seep from the seafloor in
117 many locations (MacDonald et al. 1990; Joye et al. 2005, 2009). Previous studies have
118 provided insight into the geochemical composition of these brine pools, though to date
119 volatile flux and net rates of methane oxidation remain poorly constrained due to the
120 challenges in quantification resulting from off-gassing (at *in situ* pressures and
121 temperatures relevant here, methane saturation is ~174 mmol $kg^{-1}$ (Duan and Mao,
122 2006)). Accurate sampling of fluids with high gas content using conventional methods
123 (e.g., Niskin Bottles) has thus proven impractical for volatiles.

124 The brine pool characterized in this study (AC601) is located in the Alaminos
125 Canyon lease block 601 (26º 23.53 N; 94º 30.85 W; Roberts et al. this issue; (Roberts *et*
126 *al.*, 2007). The brine pool is estimated to be ~250m in diameter and approximately 2334
127 meters below sea surface. This brine pool was visited during expeditions on board the
128 *RV Ronald H. Brown* using the *DSV Jason II* during expeditions from May 6 through
129 June 4, 2006 and June 3 through July 6, 2007 (see Roberts et al., this issue), for further
130 description of the expeditions and site locations). Discrete geochemical measurements of
131 this brine pool were made during the 2006 and 2007 expedition, while deployment of the
132 ISMS was carried out during the 2007 expedition.

## 3. Methods

### *3.1. Fundamentals of Membrane Inlet Mass Spectrometry/ISMS*

Over the past five decades, the use of membrane inlet mass spectrometry (MIMS) has proven to be a powerful tool for measuring complex mixtures of dissolved gases in both industrial and laboratory settings (Johnson *et al.*, 2000; Ketola *et al.*, 2002). MIMS represents an optimal technique for mixed environmental gas analysis, having a high degree of sensitivity and precision, with minimal sample perturbation (Kana *et al.*, 1994). MIMS has been used over the past several decades to measure and monitor a wide range of dissolved gases in aquatic and terrestrial environments, including studies of bacterial mats, peat bogs, estuarine sediments, forest soils, and tree canopies to name a few (Hemond, 1991; Kana *et al.*, 1998; Lloyd *et al.*, 1986; Lloyd *et al.*, 1998). MIMS has also been used to study metabolite flux during shipboard high-pressure experiments (e.g., (Girguis *et al.*, 2002; Girguis *et al.*, 2000). MIMS has also emerged as an important tool for analyzing dissolved gases in seawater, (e.g. dissolved gases in surface waters analyzed continuously shipboard;(Kaiser *et al.*, 2005; Tortell, 2005a; Tortell, 2005b) and more recently for *in situ* marine surface waters (Bell *et al.*, 2007; Camilli and Hemond, 2004; Kaiser *et al.*, 2005; Tortell, 2005b, c).

The recent adaptation of MIMS to *in situ* environmental analyses demonstrates the utility of such an instrument operating while underway at sea – allowing the continual monitoring of many gas species in real time. This approach allows highly accurate monitoring of spatially explicit biogeochemical changes. For example, changes in $O_2$/Ar indicate changes in net community production in ocean surface waters in different regions of the eastern equatorial Pacific (Kaiser *et al.*, 2005). Additionally, $N_2$/Ar has

156 been used to identify areas of active denitrification (e.g., $N_2$ production) in seasonally
157 oxygen-depleted bottom waters via MIMS in Saanich Inlet (Tortell, 2005b). Underway
158 shipboard trace gas analysis has also shed light on dynamics of dimethylsulfide (Tortell,
159 2005a).

160 Given the apparent utility of real-time quantification by MIMS, we aimed to
161 develop a MIMS that would achieve comparable performance in waters deeper than 1000
162 meters. Currently, investigation of deep water samples still generally requires the
163 collection of individual samples and shipboard analysis (e.g., Tortell, 2005b), risking
164 contamination and/or degassing. Furthermore, individual sample collection and analysis
165 can often result in delays between sampling and data interpretation. Our understanding
166 of deep-sea biogeochemistry would greatly benefit from real-time, *in situ* dissolved gas
167 analysis. Here we present results from a real-time *in situ* membrane inlet mass
168 spectrometer designed to A) operate at depths up to 450 atmospheres of pressure, B)
169 provide real-time data to the user (when used on human occupied submersibles or
170 remotely operated vehicles), and C) enable sampling with high spatial and temporal
171 resolution using an *in situ* pumping system.

172 ***3.2. ISMS Design and Calibration***

173 This ISMS consisted of three primary sub-systems: 1) a high-pressure membrane
174 inlet (Fig. 1a) with a small volume seawater pumping system;, 2) a quadrupole mass
175 spectrometer (Fig. 1e, f) and oil-less vacuum pumping system (Fig. 1 d, g); and 3) an
176 underwater housing (either a 2000 meter-rated aluminum 3300 alloy housing, or a 4500
177 meter rated 6AL-4V titanium housing, both of which are approximately 120 cm in length
178 and 24 cm in diameter). The membrane inlet assembly consisted of a circular sheet

179 (0.625 in. diameter) of polydimethylsiloxane (PDMS) membrane structurally backed by
180 an integrated woven fiber (Franatech, Germany). This pliable membrane material was
181 supported by a sintered stainless steel frit (5μm pore size, Applied Porous Materials,
182 Tariffville, CT), which was in turn supported by the titanium body of the inlet housing.
183 Sample water was pumped through the inlet housing assembly (2ml internal volume) at a
184 flow rate of ~3ml/min using a small solenoid pump (The Lee Company, Westbrook, CT),
185 which was controlled by an adjustable timing circuit located inside of the pressure
186 housing.

187 The membrane assembly was connected to a Stanford Research Systems Residual
188 Gas Analyzer (SRS RGA100) via standard vacuum flanges. Within the vacuum system,
189 a pressure of ~ $10e^{-5}$ Torr was maintained by a turbo-molecular pump (model: ATH 31+;
190 Alcatel, France) backed by a diaphragm roughing pump (model: ANDC83.4; KNF-
191 Neuberger, Trenton, NJ). Open source electron impact ionization was carried out with a
192 thoriated iridium wire filament. The mass spectrometer and pumps were protected from
193 membrane failure by a high-pressure / high-vacuum solenoid valve (Circle Seal, Inc.,
194 Corona, CA), which is actuated upon intrusion of water. The entire mass spectrometer
195 assembly was housed in one of the aforementioned housings. 24 VDC power and two
196 independent RS-232 channels (for serial communications with the turbo pump control
197 board and continuous feedback from the RGA analyzer) were supplied via a wet-connect
198 underwater cable (SubConn, Inc., North Pembroke, MA). In this configuration, real time
199 monitoring of fluid chemistry is achievable during submersible or ROV operations,
200 which allows for informed site selection for fluid measurements as well as adaptive
201 sampling of biological specimens.

202 To conduct the benchtop high-pressure calibrations (Fig. 2), model 110A HPLC
203 pumps (Beckman-Coulter, Fullerton, CA) were used to deliver calibrated solutions past
204 the membrane surface at various flow rates and pressures. Hydrostatic pressure against
205 the membrane inlet was manually controlled with a backpressure valve (StraVal Valve,
206 Garfield, NJ) and monitored with high pressure gauges. Various calibration solutions
207 were used including air-sparged DI water or seawater, degassed distilled water and/or
208 seawater equilibrated with gas mixtures of interest (e.g., $CH_4$), including the use of a high
209 pressure equilibration system for generating very high $CH_4$ concentrations (Fig. 2). A
210 gas chromatograph (HP 5890 Series II plus with a TCD) outfitted with a custom gas
211 extractor (Childress *et al.*, 1984) designed for quantification of rapidly degassed seawater
212 samples was used to obtain independent analyses of dissolved methane concentrations,
213 while previously described equations of state were used to calculate dissolved methane
214 concentrations at very high pressures (Duan and Mao, 2006) (Fig. 2b). During lab
215 experiments, relative changes in signal intensity were proportional to changes in the
216 permeation of gas through the membrane (either due to changes in permeate
217 concentration or changes in the permeability coefficient). We and others have observed
218 that changes in hydrostatic pressure can have an influence on permeation of gases
219 through membrane materials, in particular PDMS, interpreted to be caused by
220 compression of the membrane pore space through which analyte gas passes (Bell *et al.*,
221 2007). A change in the relationship between dissolved gas concentration and signal
222 intensity was observed during large changes in hydrostatic pressure (Fig. 2a). To account
223 for this response, we conducted calibrations using methane dissolved in seawater over a
224 range of *in situ* pressures and used these results to develop an empirical correction as

225 previously described (Bell et al., 2007). While this approach corrects for implicit
226 changes in membrane behavior, it should be noted that the ISMS dataset presented here is
227 comprised entirely of fluids sampled at a relatively constant depth (~2330m ± 2 (233
228 bar)) and temperature and as such effects due to differential pressure or temperature
229 among the samples collected were negligible. Based on benchtop calibrations, the
230 accuracy of the ISMS methane concentrations in the configuration described here was ±
231 11%, primarily due to the correction required for the pressure effects on the PDMS
232 membrane (accuracy is improved through the use of alternate membrane material (e.g.
233 Teflon AF)). Notably, however, the precision of the ISMS measurements is much better
234 than this and, based on benchtop calibrations, is within ±1%.

235 ***3.3. Water Column Methane and Oxygen Concentration***

236 To determine brine pool and seawater column methane concentrations, a CTD
237 rosette was lowered into the brine pool, using sonar to identify the brine pool as the
238 rosette approached the bottom. Niskin bottles were tripped during descent to prevent
239 contamination of bottles as gas came out of solution during the rosette's ascent. Two
240 bottles were tripped in the brine pool itself, while two were tripped 1 meter above the
241 brine-seawater interface (the interface was confirmed by the real-time conductivity
242 signal). After securing the rosette on deck, water samples were immediately transferred
243 to 1-liter PET-G bottles using gas-impermeable tubing. Bottles that were tripped in the
244 brine were substantially over-pressured and not suitable for gas quantification (though
245 samples were transferred to the PET-G bottles for rate measurements). A second sample
246 was transferred to a 250 mL BOD bottle for determination of dissolved oxygen using a
247 high sensitivity Orion® oxygen electrode. Methane was extracted using an adaptation of

248 the sonication/vacuum extraction technique (Suess *et al*., 1999) followed by gas
249 chromatography for quantification. Prior to dissolved gas extraction, samples were
250 stored at bottom water temperature (4 ºC). Two individual samples were analyzed from
251 each rosette bottle.

252 ***3.4. ISMS Deployments and Determining Brine Pool Methane Concentrations***

253 Upon reaching the brine pool, the submersible took care not to disturb the brine-
254 seawater interface. Using the ROV manipulator, the ISMS sample inlet was positioned
255 and held in place until the ISMS response reached steady state from which *in situ*
256 concentrations of $CH_4$ were calculated. A total of five independent sets of measurements
257 were made, beginning with two just above the brine fluid and three at depths of
258 approximately 5, 20 and 80 cm into the fluid (Figs. 3 and 4).

259 ***3.5. Methane Oxidation Rates***

260 Aerobic methane oxidation occurs according to the following stoichiometry:

261 $$CH_4 + 2O_2 \rightarrow HCO_3^- + H^+ + H_2O$$

262 Accordingly, aerobic methane oxidation rates were determined by incubating samples
263 with $C^3H_4$ and tracking the production of $^3H_2O$ (Carini *et al*., 2005; Valentine *et al*.,
264 2001). Typically, triplicate live and dead (Hg killed; i.e. samples were amended with
265 $HgCl_2$ to arrest all biological activity) samples from each depth were incubated for 36
266 hours at *in situ* temperatures. Unreacted $C^3H_4$ tracer was removed by purging samples
267 with water-saturated $CH_4$ and the oxidation product, $^3H_2O$, was quantified by liquid
268 scintillation counting (Carini *et al*., 2005).

In general, marine anaerobic methane oxidation in hydrocarbon seeps and brine pools is coupled to sulfate reduction, with the net reaction:

$$CH_4 + SO_4^{2-} \rightarrow HCO_3^- + HS^- + H_2O$$

Anaerobic methane oxidation rates were also determined by incubating samples with $^{14}CH_4$ and tracking the production of $^{14}CO_2$ (as in Joye *et al*., 1999; Valentine *et al*., 2001). Triplicate live and dead (Hg killed) samples from the surface (~20 cm) and sub-surface (~100 cm) brine were incubated for 48 hours at *in situ* temperatures. Unreacted $^{14}CH_4$ tracer was removed by purging with water-saturated $CH_4$ and the $^{14}CO_2$ oxidation product was quantified following acid extraction and trapping on a phethylamine wick, followed by liquid scintillation counting (Carini *et al*., 2005).

### *3.6. Sulfate Reduction Rates*

Samples for sulfate reduction were collected into gas tight glass tubes, amended with radiotracer ($^{35}SO_4^{2-}$) and incubated for 24 hours (as in Joye *et al.*, 2004; Orcutt *et al.*, 2005). For each depth, triplicate samples were incubated along side controls (killed at time zero). After incubation, samples were transferred from the tubes to 50 ml centrifuge tubes and mixed with 20% zinc acetate. Samples were processed and rates calculated as presented in Orcutt et al. (2005).

### *3.7. Major Ion chemistry*

Concentrations of major ions ($SO_4^{2-}$, $Cl^-$, dissolved inorganic carbon (DIC), dissolved organic matter (DOC and DON) and dissolved inorganic nitrogen ($NH_4^+$, $NO_2^-$ and $NO_3^-$) were determined using previously reported methods (see (Joye *et al.*, 2004) and Joye et al. this volume and references therein).

## 4. Results

### *4.1. General geochemical composition of brine pool AC601*

Geochemical data on the waters collected from the brine pool are given in Table 1. The waters of the brine pool were anoxic ($O_2$ < 2μM) with a pH of ~6.3. Salinities were substantially elevated above seawater at 82 and 92 for the 20 and 100 cm depths, respectively, with chloride measuring 1366 and 1533 mM at each depth. Water from both depths was highly enriched in dissolved inorganic carbon (DIC; 11.2 mM at 20 cm, 12.8 mM at 100 cm). Sulfate concentrations were lower than seawater, decreasing with depth into the pool (Fig 4). Dissolved inorganic nitrogen was dominated by very high $NH_4^+$ (1750 and 2195 μM, 20 and 100 cm, respectively), with $NO_3^-$ disappearing sharply in the top meter of the brine. The dissolved organic matter content was also high with a low C:N of ~4.6 suggesting the importance of autochthonous production within the brine waters.

### *4.2. Water Column and Brine Pool $CH_4$ Oxidation and $SO_4^{-2}$ Reduction Rates*

Aerobic methane oxidation rates measured in the water column above the brine pool from depths of 300m to 2313m (or heights above the brine pool from 0 to 2013m) ranged from 0.00 to 6.33 ± 0.9 pmol $L^{-1}$ $d^{-1}$ (hereafter pM $d^{-1}$) (Fig 4). The aerobic methane oxidation rate in the sample taken from directly above (~3m) the brine pool (2328m) was significantly higher, 129.6 ± 18.2 pM $d^{-1}$, than rates at any other depth. Using the methane concentrations determined via gas chromatography and the empirically derived oxidation rates, we calculate an integrated methane oxidation rate in the water column above the brine pool of 320 μmol $m^{-2}$ $yr^{-1}$

313 Within the brine pool, two samples (20cm and 100cm) were retrieved and used
314 for sulfate reduction and anaerobic oxidation of methane (AOM) rate measurements
315 (Table 2). Methane concentrations measured in the bottles used for the rate
316 measurements were 454 and 1320 μM, respectively (Table 1), giving rates at these depths
317 of 78.8 ± 7.6 and 62.1 ± 13.1 nmol $L^{-1}$ $d^{-1}$, respectively. Sulfate concentrations in the
318 brine were depleted relative to seawater with concentrations of 20 and 16mM at 20cm
319 and 100cm, respectively. Sulfate reduction rates were 107 and 50 nmoles per liter per
320 day (hereafter nM $d^{-1}$) at 20cm and 100cm, respectively, and were comparable to the rates
321 of AOM on a per mole basis. As mentioned above, these oxidation rates were measured
322 using water taken from CTD rosette bottles, which, when sampling gas-charged waters,
323 are subject to outgassing and gas phase exchange during recovery. Thus, these rates are
324 considered to be conservative estimates of anaerobic methane oxidation. *In situ* methane
325 oxidation rates are expected to be higher as methane concentrations increase (i.e., on a
326 first order basis up to $k_{max}$) and are calculated below.

327 ***4.3. Water Column and Brine Pool Methane Concentrations***

328 Methane concentrations measured in the water column (Fig 4) directly above the
329 brine pool ranged from 30nM to 70nM at depths between 2000 and 300m, representing
330 concentrations that were 15 to 32 times that of atmospheric equilibrium and underscoring
331 the transport of methane from below. At depths below 2000m, closer to the brine pool,
332 concentrations increased sharply and ranged from 111 nM to 24 μM. Methane
333 concentrations, as measured by the ISMS approximately 5 cm above the brine
334 fluid/seawater interface near the shore of the pool and 1 cm above the brine
335 fluid/seawater interface in the center of the brine pool were 180 and 590 μM,

336 respectively. Approximately 1m above the brine surface, the ISMS-measured methane
337 concentration was approximately ~35 μM, which is in general agreement with the
338 methane concentrations measured in the CTD rosette at this depth (24 μM, well below
339 the saturation of methane at one atmosphere, so these particular Niskin measurements are
340 not compromised by off gassing, see Fig. 4). Concentrations at depths of 5, 20 and 80cm
341 into the brine fluid near the center of the pool were orders of magnitude higher (Fig 4)
342 with values of 14.3, 20.3 and 33.3 mM, respectively (± 2%), and more than an order of
343 magnitude in excess of concentrations measured with Niskin sampling (see Table 1).

344 **5. Discussion**

345 ***5.1. In situ rates of brine pool anaerobic methane oxidation***

346 The *in situ* rates of AOM reported here exceed values in other anoxic waters by at
347 least one to two orders of magnitude. Our measured rates of AOM from two sampling
348 depths allowed calculation of first order rate constants of 0.063 and 0.017 $yr^{-1}$ from
349 depths of 20cm and 80cm, respectively. Coupling the *in situ* methane concentration
350 measurements from the ISMS to the aforementioned rate constants yields estimates of the
351 actual rates of AOM of 1285 ± 125 and 572 ± 121 μM $yr^{-1}$ at the depths of 20 and 80cm
352 in the brine pool, respectively. To the best of our knowledge, these AOM rates are by far
353 the highest documented in an anoxic water body. Whereas there has been some evidence
354 that AOM is inhibited by high chloride concentrations (e.g.,(Joye *et al.*, 2009; Oren,
355 2002)), our data (Tables 1 and 2) suggest that moderately high salinities may in fact not
356 be inhibitory to AOM and that coupled sulfate reduction and AOM may yet play an
357 important role in many Gulf of Mexico hydrocarbon/brine environments.

358 Many studies have measured AOM in deep sea environments with high
359 concentrations of methane, and the highest rates are generally found within sediments,
360 particularly hydrate-influenced sediments (e.g., (Devol, 1983; Girguis *et al.*, 2003; Joye
361 *et al.*, 2004; Reeburgh, 1980)). Indeed, far fewer studies have measured AOM occurring
362 in anoxic water columns, and the rates reported in these studies are generally much lower
363 than sediment rates (as is the case with most biogeochemical processes primarily due to
364 microbial density being substantially higher in sediments). Rates of AOM measured in
365 the anoxic waters of the Cariaco Basin (~1.5 μM $yr^{-1}$; Ward *et al.*, 1987), Saanich Inlet
366 (7.3 μM $yr^{-1}$; Ward *et al.*, 1989) and the Black Sea (0.6 μM $yr^{-1}$; Reeburgh *et al.*, 1991)
367 were all orders of magnitude lower than those observed in this study. Joye et al (1999)
368 measured rates as high as 17.5 μM $yr^{-1}$ in the bottom waters of alkaline, saline Mono
369 Lake. Notably, these rates were measured during a period when the lake waters were
370 well mixed. More recent data collected during a period of extended meromixis in Mono
371 Lake exhibit substantially higher rates of AOM (up to 365 μM $yr^{-1}$) (Joye *et al.*,
372 submitted).
373 The rates of AOM presented here are also consistent with the extremely high *in*
374 *situ* concentrations occurring at these depths. Turnover times of methane in the anaerobic
375 brines were on the order of 16 to 58 years, more than long enough to maintain supply of
376 $SO_4^{-2}$ via diffusion. Such long turnover times also might suggest that supply to the
377 overlying water via diffusion is likely to be a substantial methane sink relative to removal
378 by AOM (or aerobic oxidation at the brine-seawater interface) in similar brine pool
379 environments. Indeed, given that the rate constants were lower than many other
380 comparable environments, the rates presented represent a conservative estimate and, as

381 previously mentioned, the rate constants would likely increase at the higher methane
382 concentrations found *in situ*.

383 ***5.2. Estimates of $CH_4$ flux from the brine pool***

384 Research on deep-sea fluxes and transformations of biological compounds is
385 constantly challenged by the need to sample at extreme temperatures, depths and
386 pressures. Measurement of these compounds *in situ* provides more rigorous constraints
387 on their fluxes and transformation rates. In the context of the current study, the *in situ*
388 mass spectrometer allowed direct measurement of methane concentrations in a gas-
389 charged brine pool. These concentration measurements were used to calculate a diffusive
390 flux of methane from the brine pool into the overlying water column of $1.1 \pm 0.2$ mol $m^{-2}$
391 $yr^{-1}$, illustrating the magnitude of methane flux from benthic environs into the overlying
392 mixed layer (discussed in detail below).

393 Specifically, discrete *in situ* measurements taken over a depth profile across the
394 seawater-brine interface provide a context for calculating diffusive geochemical fluxes of
395 methane into the overlying water column. This approach has been used in numerous
396 studies for estimating the mass transfer (e.g., fluxes) of solutes from one region into
397 another. Brine pools such as AC601 are generally very quiescent in nature with fluid
398 advection playing a small role in controlling fluxes (Joye *et al.*, 2005; Joye *et al.*, 2009).
399 In these locations, where diffusion is the dominant mode of mass transfer, Fick's first law
400 is used to make first order estimates of the diffusive flux based on the measured
401 concentration gradients. The range of possible flux values is estimated based on error in
402 the spatial resolution of the gradient (i.e., since high precision positioning of the sampling
403 wand was not possible, we estimate the potential vertical position ± 10cm). Moreover,

404 we adopted a value of $1.38e^{-5}$ $cm^2$ $s^{-1}$ for the diffusion coefficient of methane in seawater
405 adjusted for the average viscosity of the brine using the Stokes-Einstein relationship
406 (Mao and Duan, 2008; Sahores and Witherspoon, 1970).
407 Even with our lower-bound estimate of diffusive methane flux (1.1 mol $m^{-2}$ $yr^{-1}$),
408 water column integrated methane oxidation rates (Fig. 4) measured directly above the
409 brine pool (~320 μmol $m^{-2}$ $yr^{-1}$) indicate that only a very small fraction of methane
410 escaping the brine pool is biologically consumed in the overlying water column (0.02 to
411 0.03%). While it is likely that lateral advection plays a large role in the disconnect
412 between brine pool flux and water column methane oxidation rates above the brine, upper
413 water column concentrations are nonetheless >10 times that of methane in equilibrium
414 with the atmosphere, confirming the transport of methane from depths >2000m into the
415 mixed layer which easily escapes, un-oxidized, into the atmosphere.
416 Our estimates of diffusive methane flux should be taken as a lower bound on flux
417 from environments such as Gulf of Mexico brine pools. They also underscore the value
418 of *in situ* measurement for constraining methane fluxes. For example, other studies
419 (Lapham *et al.*, 2008; Schmidt *et al.*, 2003) have modeled diffusive and/or advective
420 fluxes from brine seep environments by comparing profiles of a non-conservative solute
421 (e.g., methane) to conservative solutes (e.g., chloride, temperature). Using a 1-D reaction
422 transport model together with chloride and methane profiles, advective methane fluxes of
423 up to 2 mol $m^{-2}$ $yr^{-1}$ were estimated from brine-influenced sediments characterized by a
424 strong advective flow (Lapham *et al.*, 2008). However, these calculated fluxes were
425 based on methane concentrations from sediment cores that had degassed upon collection,
426 and were thus substantially lower than methane concentrations *in situ*. In another study,

Solomon et al. (2008) employed osmotic samplers demonstrating that net seafloor methane fluxes range from 0.89 mol $m^{-2}$ $yr^{-1}$ from a mussel bed environment up to 29 mol $m^{-2}$ $yr^{-1}$ from a bacterial mat environment. Hereto, because methane concentrations could not be reliably determined at *in situ* pressure and temperature, fluxes were calculated assuming that porewater was in equilibrium with methane hydrate under *in situ* conditions. However, others have shown that methane in sediments around hydrate can be far from saturated (Lapham *et al.*, pers. comm.), which would result in much lower flux estimates. Future studies should aim to couple *in situ* methane measurements with direct fluid flow measurements to better constrain the contribution of adjective flux to water column methane flux.

## 6. Summary and Conclusions

Our calculated *in situ* AOM rates, using empirically derived rate constants, are higher than those previously published by one to two orders of magnitude. The diffusive flux was estimated to range as high 1.8 mol $m^{-2}$ $yr^{-1}$ from the brine pool, while integrated oxidation rates in the overlying 2000m water column could only account for 0.32 μmol $m^{-2}$ $yr^{-1}$. These data suggest that a very large component of the diffusive brine pool methane flux escapes both aerobic and anaerobic oxidation in the water column above the brine pool and may be released into the atmosphere (or at least subject to dispersion via lateral advection). These first *in situ* measurements of methane concentration from a brine pool using the ISMS enabled robust quantification of methane concentrations at *in situ* conditions in these gas-charged brines and reflect the strong influence of the surrounding hydrocarbon seep environments. Such integrated approaches – wherein geochemical determinations are coupled with microbiological activity measurements –

450 are the best means of providing a rigorous constraint on methane diffusive fluxes and
451 transformation rates. This will improve our understanding of the role that hydrocarbon
452 seeps may play in the delivery of methane into the ocean and ultimately the atmosphere.
453

**Acknowledgements**

We are especially grateful to Stephane Hourdez for his immense help with this instrument during this expedition. We are also grateful to Dr. Charles Fisher for his support, as well as the captains and crew of the *RV Ronald H. Brown* and *RV Atlantis*. Special thanks to the pilots and support staff of the *DSV ALVIN* and *DSV JASON II* from Woods Hole Oceanographic Institution for help collecting and processing samples. An extra thanks goes especially to Matthew Heinz and Tito Collasius for their assistance in the machine shop. This research was supported by the U.S. Department of the Interior Minerals Management Service, the National Oceanic and Atmospheric Administration, the David and Lucile Packard Foundation, Harvard University, and the National Science Foundation (MCB-0702504).

**Figure captions**

**Figure 1:** Schematic of the in situ mass spectrometer. a) membrane inlet housing, b) front end plate of titanium pressure housing, c) high pressure solenoid for isolation of vacuum chamber, d) Alcatel ATH-31+ Turbo Pump, e) vacuum flight tube housing the SRS Quadrupole RGA-200 including ion source, quadrupoles and detectors f) electronics head for controlling and reading spectrometer signals g) KNF Neuberger roughing pump model ANDC-84.3. Sample gas is continuously extracted across the membrane located in (a) into the high vacuum system (d, g), ionized in (e) and analyzed by the detector and electronics control unit housed in (f). The instrument is approximately 1m in length.

**Figure 2:** a) Normalized response at m/z 15 over a range of hydrostatic pressure for three example fluid temperatures and concentrations, 10˚C 1160μM $CH_4$ (grey squares), 2˚C 800 μM $CH_4$ (black triangles) and 14˚C 180 μM $CH_4$ (grey triangles). Responses to pressure were experimentally fit under a wide range of temperatures and concentrations (as in Bell et al 2007) with values of b' ranging between 0.02 to 0.24 and values of k ranging between 0.84 to 0.94. b) The response of m/z 15 (corrected for pressure effects – see Fig 2a) was linearly proportional to methane concentrations as measured independently by gas chromatography (grey triangles) and as calculated after Duan et al 2006 during high pressure calibration measurements (black circles).

**Figure 3**: Photo from the Pilot Cam of ROV Jason showing the starboard manipulator reaching through the seawater/brine pool interface and sampling at a depth of approximately 80cm.

**Figure 4**: a) Depth profile of methane concentration and methane oxidation rates in the water column above brine pool AC601. Note log scale. Open circles are concentration measurements made from Niskin bottle samples, while black circles are those made *in situ* using the ISMS. b) Close-up of seawater/brine pool interface and profile into the brine fluid. Note the linear scale in contrast to panel a. Measured rates of anaerobic methane oxidation (AOM) at two depths within the brine pool are shown. Note that these, when corrected for in situ CH4 concentrations, these rates are 30-45 times higher. Sulfate concentrations are depleted in the brine, consistent with its role in AOM.

## References


Bell, R.J., Short, R.T., van Amerom, F.H., Byrne, R.H., 2007. Calibration of an In Situ Membrane Inlet Mass Spectrometer for Measurements of Dissolved Gases and Volatile Organics in Seawater. Environmental Science & Technology 41 (23), 8123-8128.

Camilli, R., Hemond, H.F., 2004. NEREUS/Kemonaut, a mobile autonomous underwater mass spectrometer. Trends in Analytical Chemistry 23 (4), 307-313.

Carini, S., LeCleir, G., Bano, N., Joye, S.B., 2005. Acitivity, abundance and diversity of aerobic methanotrophs in an alkaline, hypersaline lake (Mono Lake, CA, USA). Environmental Microbiology 7 (8), 1127-1138.

Childress, J.J., Arp, A.J., Fisher Jr., C.R., 1984. Metabolic and blood characteristics of the hydrothermal vent tubeworm Riftia pachyptila. Marine Biology 83, 109-124.

Collett, T., Kuuskraa, V., 1998. Hydrates contain vast store of world gas resources. Oil Gas Journal 96 (19), 90-95.

Devol, A.H., 1983. Methane oxidation rates in the anaerobic sediments of Saanich Inlet. Limnology and Oceanography 28, 738-742.

Dickens, G.R., 2003. Rethinking the global carbon cycle with a large, dynamic and microbially mediated gas hydrate capacitor. Earth and Planetary Science Letters 213 (3-4), 169-183.

Duan, Z., Mao, S., 2006. A thermodynamic model for calculating methane solubility, density and gas phase composition of methane-bearing aqueous fluids from 273 to 523K and from 1 to 2000 bar. Geochimica et Cosmochimica Acta 70 (13), 3369-3386.

Fisher, C.R., Roberts, H., Cordes, E.E., Bernard, B., 2007. Cold seeps and associated communities of the Gulf of Mexico Oceanography 20 (4), 118-129.

Girguis, P.R., Childress, J.J., Freytag, J.A., Klose, K., Stuber, R., 2002. Effects of metabolite uptake on proton-equivalent elimnation by two species of deep-sea vestimentiferan tubeworms, *Riftia pachyptila* and *Lamellibrachia luymesi*. Journal of Experimental Biology 205, 3005-3006.

526 Girguis, P.R., Lee, R.W., Childress, J.J., Pospesel, M., Desaulniers, N.T., Zal, F.,
527 Felbeck, H., 2000. Fate of nitrate acquired by the hydrothermal vent tubeworm
528 *Riftia pachyptila*. Applied and Environmental Microbiology 66 (7), 2783-2790.
529 Girguis, P.R., Orphan, V.J., Hallam, S.J., DeLong, E.F., 2003. Growth and methane
530 oxidation rates of anaerobic methanotrophic archaea in a continuous flow reactor
531 bioreactor. Applied and Environmental Microbiology 69, 5492-5502.
532 Hemond, H.F., 1991. A Backpack-portable mass spectrometer for measurement of
533 volatile compounds in the environment. Review of Scientific Instruments 62 (6),
534 1420-1425.
535 Johnson, R., Cooks, R., Allen, T., Cisper, M., Hemberger, P., 2000. Membrane
536 introduction mass spectrometry: Trends and applications Mass Spectrometry
537 Reviews 19, 1-37.
538 Joye, S.B., Boetius, A., Orcutt, B.N., Montoya, J.P., Schulz, H.N., Erickson, M.J., Lugo,
539 S., 2004. The anaerobic oxidation of methane and sulfate reduction in sediments
540 from Gulf of Mexico cold seeps. Chemical Geology 205, 219-238.
541 Joye, S.B., Connell, T.L., Miller, L.G., Oremland, R.S., Jellison, R.S., 1999. Oxidation of
542 ammonia and methane in an alkaline, saline lake. Limnology and Oceanography
543 44 (1), 178-188.
544 Joye, S.B., MacDonald, I.R., Montoya, J.P., Peccini, M., 2005. Geophysical and
545 geochemical signatures of Gulf of Mexico seafloor brines. Biogeosciences 2, 295-
546 309.
547 Joye, S.B., Samarkin, V., Orcutt, B.N., MacDonald, I.R., Hinrichs, K.-U., Elvert, M.,
548 Teske, A., Lloyd, K.G., Lever, M.A., Montoya, J.P., Meile, C., 2009. Metabolic
549 variability in seafloor brines revealed by carbon and sulfur cycling. Nature
550 Geosciences 2, 349-354.
551 Kaiser, J., Reuer, M.K., Barnett, B., Bender, M.L., 2005. Marine productivity estimates
552 from continuous O2/Ar ratio measurements by membrane inlet mass
553 spectrometry. Geophysical Research Letters 32, doi:10.1029/2005GL23459.
554 Kana, T.M., Darkangelo, C., Hunt, M.D., Oldham, J.B., Bennett, G.E., Cornwell, J.,
555 1994. Membrane Inlet Mass Spectrometer for Rapid High-Precision

556 Determination of N2, O2, Ar in Environmental Water Samples. Analytical
557 Chemistry 66, 4166-4170.
558 Kana, T.M., Sullivan, M.B., Cornwell, J.C., Groszkowski, K.M., 1998. Denitrification in
559 estuarine sediments determined by membrane inlet mass spectrometry.
560 Limnology and Oceanography 43 (2), 334-339.
561 Kennicutt, M.C., II, Brooks, J.M., Denous, G., 1988. Leakage of deep, reservoired
562 petroleum to the near surface on the Gulf of Mexico continental slope. Marine
563 Chemistry 24, 29-59.
564 Ketola, R.A., Kotiaho, T., Cisper, M.E., Allen, T.M., 2002. Environmental applications
565 of membrane introduction mass spectrometry. Journal of Mass Spectrometry 37,
566 457-476.
567 Kvenvolden, K., 1993. Gas hydrates - geological perspective and global change. Reviews
568 of Geophysics 31 (2), 173-187.
569 Kvenvolden, K., Lorensen, T.D., 2008. A global inventory of natural gas hydrate
570 occurence. http://walrus.wr.usgs.gov/globalhydrate/index.html.
571 Lapham, L.L., Alperin, M., Chanton, J., Martens, C.S., 2008. Upward advection rates and
572 methane fluxes, oxidation, and sources at two Gulf of Mexico brine seeps. Marine
573 Chemistry 112, 65-71.
574 Lloyd, D., Davies, K.J., Boddy, L., 1986. Mass spectrometry as an ecological tool for in
575 situ measurement of dissolved gases in sediment systems. FEMS Microbiology
576 Ecology 38, 11-17.
577 Lloyd, D., Thomas, K.L., Hayes, A., Hill, B., Hales, B.A., Edwards, C., Saunders, J.R.,
578 Ritchie, D.A., Upton, M., 1998. Micro-ecology of peat: Minimally invasive
579 analysis using confocal laser scanning microscopy, membrane inlet mass
580 spectrometry and PCR amplification of methanogen-specific gene sequences.
581 FEMS Microbiology Ecology 25, 179-188.
582 MacDonald, I.R., Reilly, J., Guinasso, J., Brooks, J.M., Carney, R., Bryant, W.A., Bright,
583 T.J., 1990. Chemosynthetic mussels at a Brine-filled pockmark in the Northern
584 Gulf of Mexico. Science 248 (4959), 1096-1099.

585 MacDonald, I.R., Sager, W., Peccini, M., 2003. Association of gas hydrate and
586 chemosynthetic fauna in mounded bathymetry at mid-slope hydrocarbon seeps:
587 Northern Gulf of Mexico. Marine Geology 198, 133-158.
588 Orcutt, B.N., Boetius, A., Elvert, M., Samarkin, V., Joye, S.B., 2005. Molecular
589 biogeochemistry of sulfate reduction, methanogenesis and the anaerobic oxidation
590 of methane at Gulf of Mexico cold seeps. Geochimca et Cosmochimica Acta 69
591 (17), 4267-4281.
592 Oren, A., 2002. Diversity of halophilic microorganisms: environments, phylogeny,
593 physiology, and applications. Journal of Industrial Microbiology and
594 Biotechnology 28, 56-63.
595 Reeburgh, W.S., 1980. Anaerobic methane oxidation: Rate depth distribution in Skan
596 Bay sediments. Earth and Planetary Science Letters 47 (3), 345-352.
597 Reeburgh, W.S., 2007. Oceanic Methane Biogeochemistry. Chemical Reviews 107 (2),
598 486-513.
599 Roberts, H., Carney, R., 1997. Evidence of episodic fluid, gas, and sediment venting on
600 the northern Gulf of Mexico continental slope Economic Geology 92, 863-879.
601 Roberts, H., Fisher, C.R., Bernard, B., Brooks, J.M., Bright, M., Carney, R., Cordes, E.,
602 Hourdez, S., Hunt, J.J., Joye, S.B., 2007. ALVIN explores the deep northern Gulf
603 of Mexico Slope. Eos Transactions 88, 341-342.
604 Schmidt, M., Botz, R., Faber, E., Schmitt, M., Poggenburg, J., Garbe-Schönberg, D.,
605 Stoffers, P., 2003. High-resolution methane profiles across anoxic brine-seawater
606 boundaries in the Atlantis-II, Discovery, and Kebrit Deeps (Red Sea). Chemical
607 Geology 200, 359-375.
608 Sloan, L.C., Walker, J.C., Moore, J., TC, Rea, D.K., Zachos, J.C., 1992. Possible
609 methane-induced polar warming in the early Eocene Nature 357, 320-322.
610 Solomon, E.A., Kastner, M., Jannasch, H., Robertson, G., Weinstein, Y., 2008. Dynamic
611 fluid flow and chemical fluxes associated with a seafloor gas hydrate deposit on
612 the northern Gulf of Mexico slope. Earth and Planetary Science Letters 270, 95-
613 105.
614 Suess, E., Torres, M., Bohrmann, G., Collier, R., Greinert, J., Linke, P., Rehder, G.,
615 Trehu, A., Wallman, K., Zuleger, E., 1999. Gas hydrate destablization: Enhanced

dewatering, benthic material turnover and large methane plumes at the Cascadia convergent margin. Earth and Planetary Science Letters 170, 1-15.

Tortell, P., 2005a. Small-scale heterogeneity of dissolved gas concentrations in marine continental shelf waters. Geochemistry, Geophysics, Geosystems 6, Q11M04.

Tortell, P.D., 2005b. Dissolved gas measurements in oceanic waters made by membrane inlet mass spectrometry. Limnology and Oceanography: Methods 3, 24-37.

TValentine, D.L., Blanton, D., Reeburgh, W.S., Kastner, M., 2001. Water column methane oxidation adjacent to an area of active hydrate dissociation, Eel River Basin. Geochimca et Cosmochimica Acta 65, 2633-2640.

Zachos, J.C., Pagani, M., Sloan, L., Thomas, E., Billups, K., 2001. Trends, rhythms and aberrations in global climate 65 Ma to Present. Science 292 (5517), 686-674.

**Table 1: Major chemical components of brine pool AC601**

| | | | | Concentration mM | | | | | | Concentration mM | | | | | | |
|---|---|---|---|---|---|---|---|---|---|---|---|---|---|---|---|---|
| **Depth cm** | **pH** | **salinity** | **oxygen** | **DIC** | **$H_2S$** | **$SO_4^{-2}$** | **$Cl^-$** | **$CH_4$[a]** | **$CH_4$[b]** | **$NH_4^+$** | **$NO_x$** | **DIN** | **TDN** | **DON** | **DOC** | **DOC:DON** |
| **5** | | | | | | | | | 14.35 | | | | | | | |
| **20** | 6.29 | 82 | <2 µM | 11.2 | 0.00 | 20 | 1366 | 0.454 | 20.29 | 1750 | 3.4 | 1753.4 | 1843.5 | 90.1 | 423.5 | 4.7 |
| **80** | | | | | | | | | 33.29 | | | | | | | |
| **100** | 6.25 | 92 | <2 µM | 12.8 | 0.25 | 16 | 1533 | 1.320 | 38.40* | 2195 | 0.3 | 2195.3 | 2280.5 | 85.2 | 380.0 | 4.5 |

[a]Concentrations measured via gas chromatography on samples retrieved with a CTD rosette and Niskin bottles

[b]Concentrations measured via *in situ* mass spectrometer

* estimated by regression of the three ISMS data points collected above

635
636
637

**Table 2: Rates of sulfate reduction and anaerobic methane oxidation in Gulf of Mexico brine pool AC601**

| | Rate nM/d | | | | | | | | |
|---|---|---|---|---|---|---|---|---|---|
| **Depth cm** | **Sulfate Reduction** | | | **Anaerobic Methane Oxidation*** | | | **Anaerobic Methane Oxidation^** | | |
| **20** | 107.1 | ± | 14.6 | 78.8 | ± | 7.6 | 3502.0 | ± | 340 |
| **100** | 49.8 | ± | 8.4 | 62.1 | ± | 13.1 | 1807.4 | ± | 330 |

***** measured using water samples collected via CTD rosette and Niskin bottles
^ estimated rates corrected for measured concentrations*in situ* and using rate constants measured from shipboard incubations of brine pool water collected via Niskin bottles

638
639
640
641
642
643

643

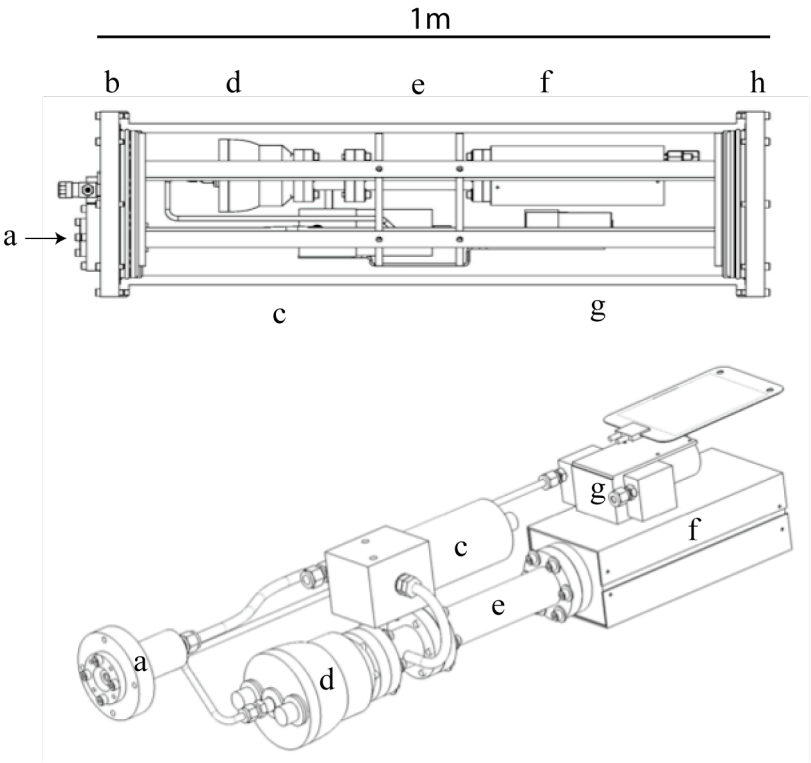


Wankel Figure 1

644

645

646

647

648

649

649

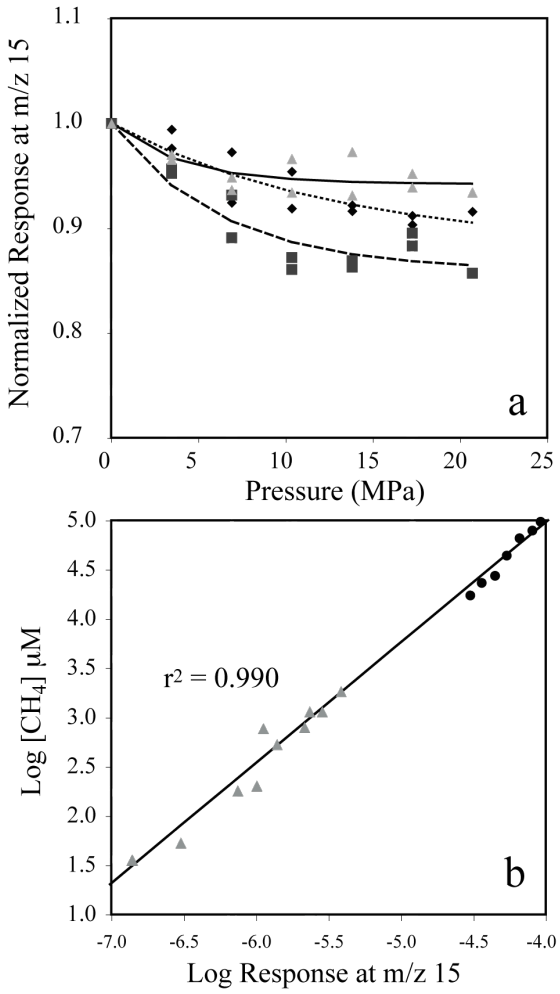


650

Wankel Figure 2

651

652

# Wankel Figure 3

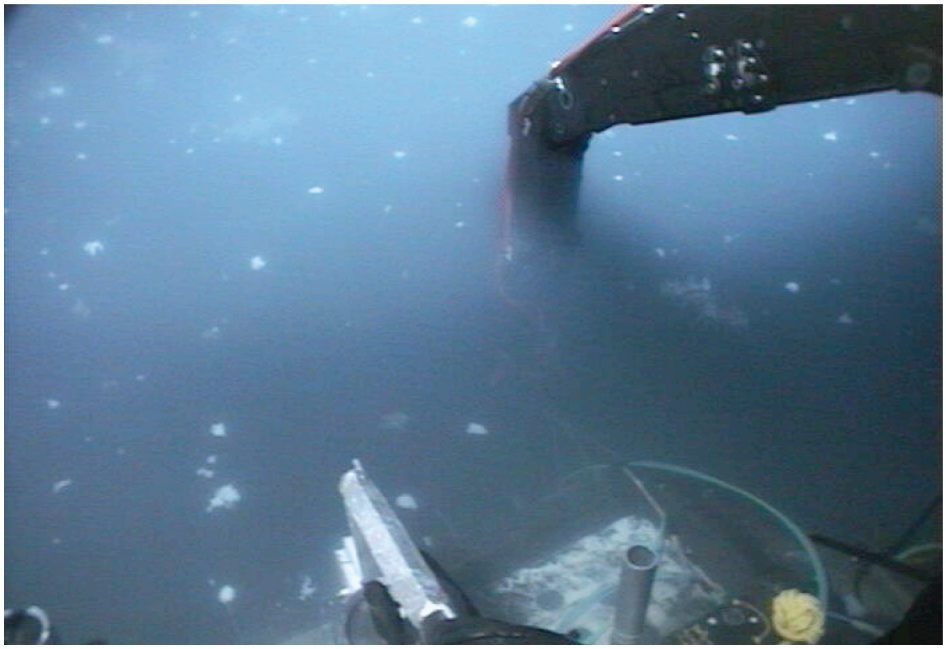

653

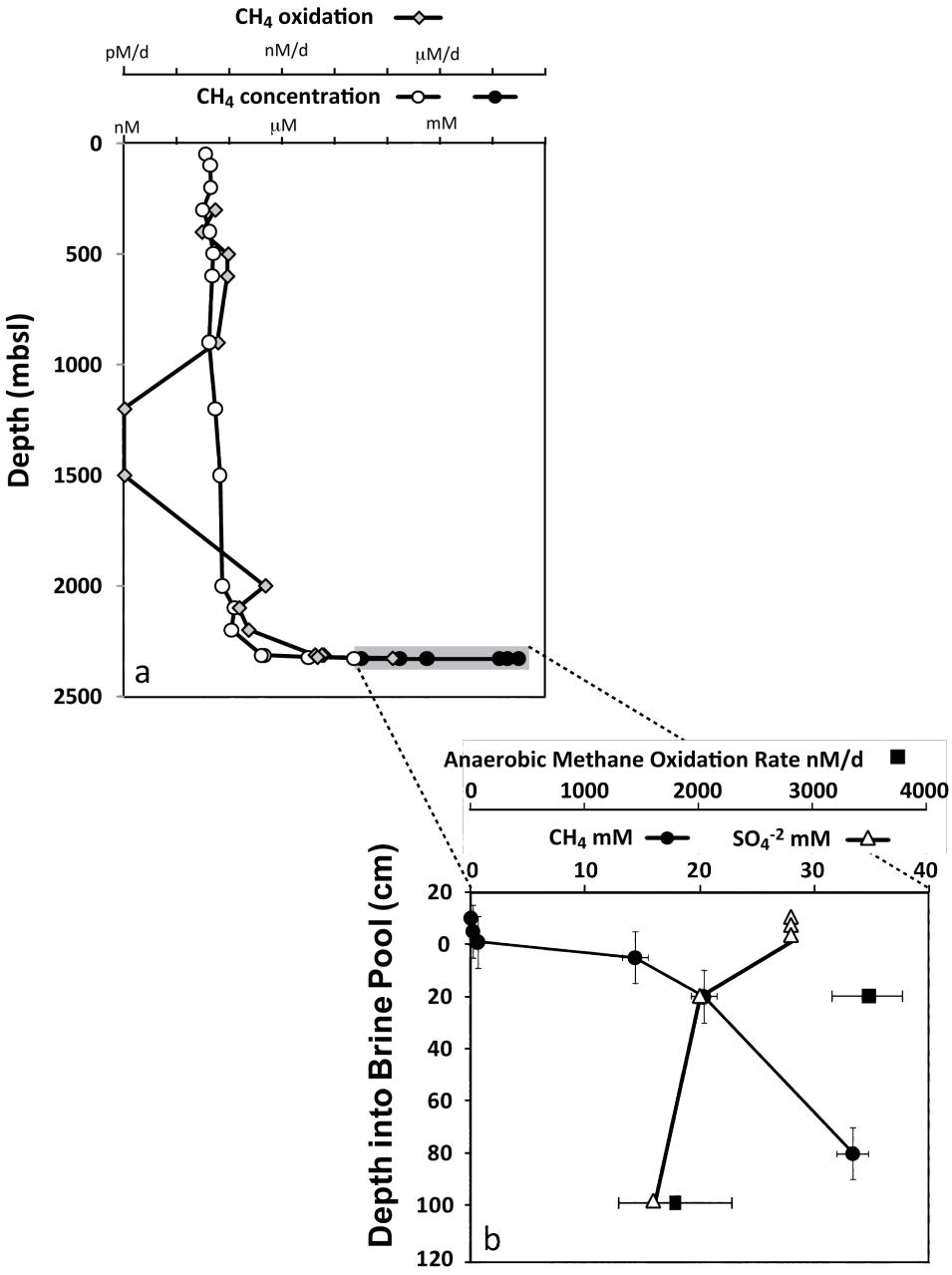


Wankel Figure 4

654

655

656